UNITED STATES DEPARTMENT OF THE INTERIOR

GEOLOGICAL SURVEY

Airborne Radiometric and Magnetic Survey of Parts of the Upper Peninsula of Michigan and northern Wisconsin

By

U.S. Geological Survey

In cooperation with

U.S. Department of Energy

and Michigan Technical University

Open File Report 83-195-A

1983

Introduction

by

William D. Heran

The data presented in this report are from an airborne reconnaissance gamma-ray and total-field magnetic survey conducted by High Life Helicopters Inc. and its subsidiary QEB Inc., for the U.S. Geological Survey. The survey is located in four areas in the Upper Peninsula of Michigan. Jacobsville (sub-areas A1-A5), Northern CUSMAP (Area B), Limestone Mountain (Area C), Sylvania Wilderness (Area D), and one wilderness area in northern Wisconsin, (Area E) (fig. 1). All of the areas except area E (fig. 1) are within the Iron River 1^{o} X 2^{o} quadrangle. This quadrangle was being studied as part of the U.S. Geological Survey (USGS) CUSMAP (Conterminous United States Mineral Appraisal Program) project. (Cannon, 1982), (U.S. Geological Survey, 1982). The survey was done in order to provide geophysical information to aid in the mineral resource evaluation of the Iron River 1^{o} X 2^{o} quadrangle, to provide information to the U.S. Department of Energy on potential uranium deposits and to provide information needed in the mineral evaluation of wilderness areas.

Specific objectives for each of the areas are as follows. Areas A-1 through A-5 were flown over the contact between Proterozoic Jacobsville Sandstone and older crystalline basement rock, a geologic setting thought to be favorable for uranium mineralization (Kalliokoski, 1977). The funding for the collection of geophysical data in area A was provided by the U.S. Department of Energy as a part of their study of uranium deposits.

Area B (fig. 1) comprises part of a gneissic dome complex (Cannon, 1978) that includes metavolcanic, graphitic, gneiss, iron formation and metasedimentary units. The survey was flown because there are known uranium and basemetal occurrences in this area. Funding for the survey was provided through the USGS CUSMAP project.

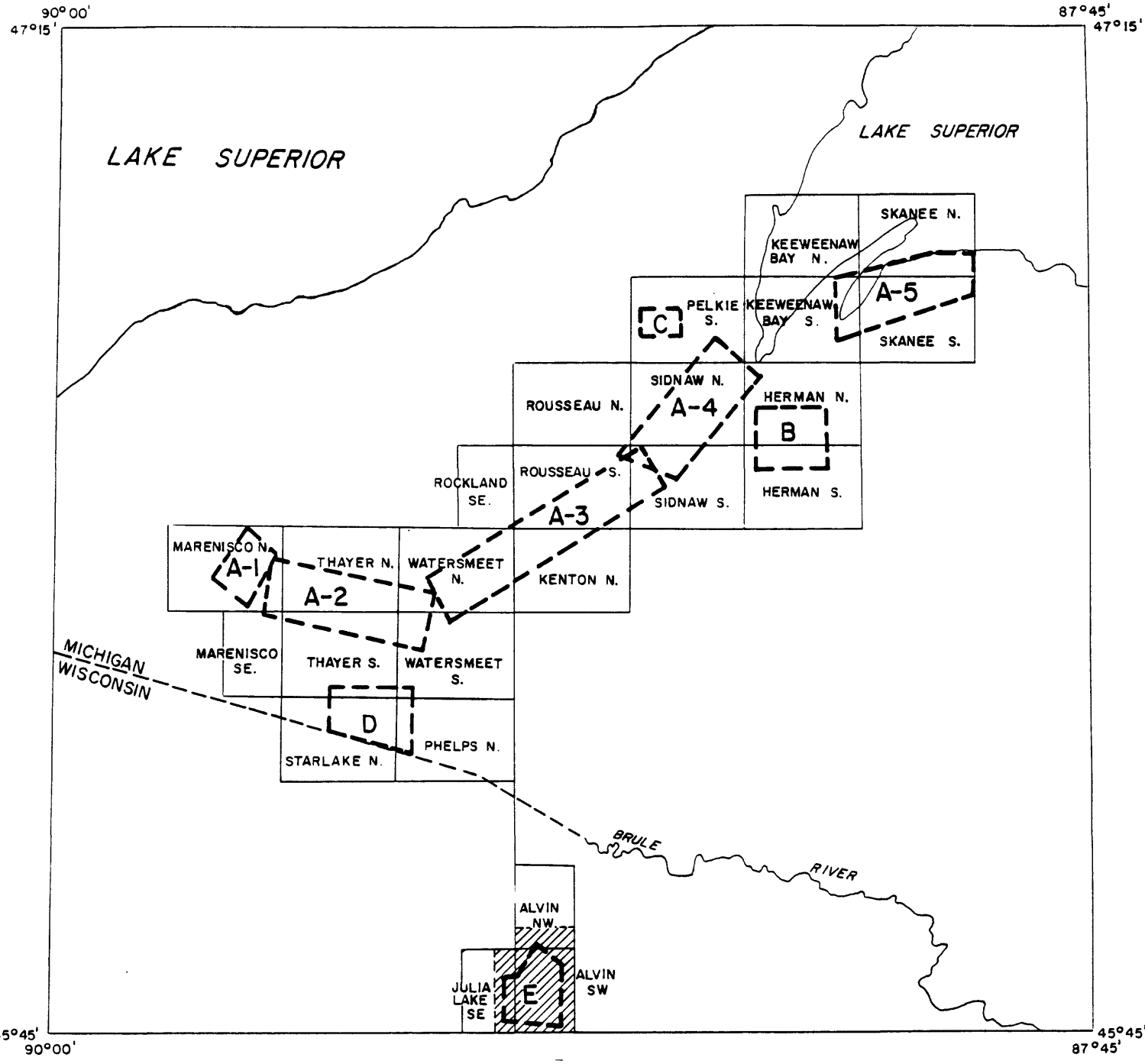

LOCATION DIAGRAM

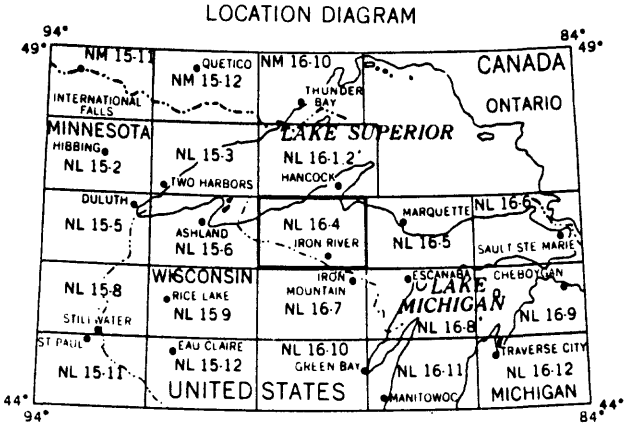

Scale 1:1,000,000
1 inch equals approximately
16 miles

0 10 20miles

Figure 1.
Location of survey areas

Area C (fig. 1) is a region of structural complexity within the Jacobsville Sandstone that was being studied and funded jointly by the USGS CUSMAP project and the Geology Department at Michigan Technical University at Houghton, Michigan. (Ensign, P. S., 1981).

Areas D and E (fig. 1) are wilderness study areas. Flying in these areas was funded by the USGS Wilderness program.

General Discussion of Gamma Radiation and Instrumentation

The gamma radiation that is measured in an airborne survey includes background radiation from atomospheric sources and radiation originating within a thin layer at and beneath the ground surface. Soil, rock, and water effectively attenuate gamma radiation. Approximately 90 percent of the measured radiation, which originates beneath the ground surface, comes from the upper 0.3 m of soil or 0.7 m of water (Bailey and Childers, 1977).

The measuring unit consists of one or more crystals of thallium-activated sodium iodide, a material which emits a flash of light (scintilation) when hit by a gamma ray. The intensity of scintilation is directly proportional to the energy of the gamma ray, which is a measurable function of the uranium, thorium, or potassium source. The scintilation is converted to a voltage, by a photomultiplier tube, and the pulse height is compared with that of a reference source. Voltage pulses are fed into separate diagnostic channels for uranium, thorium and radiopotassium and into a total-count channel which shows the number of gamma rays arriving per second within a particular energy range (Peters, 1978).

Gamma radiation that has energies sufficient to penetrate 100 to 200 m of air and be detected by a sodium-iodide crystal is given off by the decay of several isotopes of the uranium and thorium decay series, as well as of

potassium. For aerial gamma-ray surveys, bismuth-214 (^{214}Bi) is the important gamma emitter for the uranium series and thallium-208 (^{208}Tl) is the important emitter for the thorium series. Uranium, thorium, and potassium gamma rays are high-energy photons (Adams and Gasparini, 1970) whose energies range from several KeV (thousand electron volts) to 2.8 MeV (million electron volts). The energies of the three important gamma rays, are 1.46 MeV (^{40}K) for potassium, 1.76 MeV (^{214}Bi) for uranium, and 2.62 MeV for thorium (^{208}Tl).

Window spectrometers are used in most airborne surveys, and are designed with four windows to count photons that have the energies of interest. More sophisticated is the multichannel spectrometer that defines the full spectrum. A gamma-ray spectrometric survey has several advantages over total gamma radiation survey. First, uranium and thorium can be differentiated when both are present in significant amounts. Also, isotope-ratio maps can be produced from the data. Surface topography and other factors can produce weak anomalies in ^{214}Bi or ^{208}Tl, but the ratio of $^{214}Bi/^{208}Tl$ is only affected by real differences in one isotope relative to the other when elevation variations are corrected (Bailey and Childers, 1977).

For information concerning the interpretation of Airborne Radiometric data the reader may refer to (Saunders, and Potts 1978).

Following this introduction is a report prepared by High Life Helicopters Inc./QEB, Inc. for the U.S. Geological Survey. This report is one of two open-file reports and is accompanied by combined magnetic interpretation and uranium anomaly maps (total of 46 in all), which were plotted on flight line maps prepared on a 1:24,000 scale topographic base. The other report (U.S. Geological Survey 1983) contains the stacked profiles of all data. The material in this report is the sole responsibility of the contractor. It does not necessarily express the view of the U.S. Geological Survey.

The radiometric and magnetic data for these areas is supplemented by an airborne electromagnetic and magnetic survey. (Geoterrex Limited, with an introduction by W. D. Heran, 1981).

The survey areas correspond to the following plates listed. Plates are numbered right to left, top to bottom according to longitude and latitude position of plate.

Area	Plate
Jacobsville A-1	1-2
Jacobsville A-2	3-10
Jacobsville A-3	11-21
Jacobsville A-4	22-28
Jacobsville A-5	29-33
Northern Cusmap B	34-37
Limestone Mtn. C	38
Sylvania Wilderness D	39-43
Wisconsin Wilderness E	44-46

References Cited

Adams, J. A. S., and Gasparini, 1970, Gamma-ray spectrometry of rocks: Amsterdam, Elsevier, 295 p.

Bailey, R. V. and Childers, M. O., 1977, Applied mineral exploration with special reference to uranium: Westview Press, 513 p.

Cannon, W. F., 1978, Geologic map of the Iron River 1^{o} x 2^{o} quadrangle, Michigan and Wisconsin: U.S. Geological Survey Open File Report 78-342, scale 1:250,000.

_____, 1982, Mineral Resource Assessment of the Iron River 1^{o} X 2^{o} Quadrangle, Michigan and Wisconsin, U.S. Geological Survey Open-File 82-223, 33p.

Ensign, P. S., 1981, An INPUT Electromagnetic Investigation of the southern margin of the Jacobsville Sandstone, Upper Penninsula of Michigan: Houghton, Michigan Technological University, M.S. Thesis, 66 p.

Geoterrex Ltd., With an introduction by Heran, W. D., 1981, Airborne Electromagnetic and Magnetic Survey of parts of the Upper Peninsula of Michigan and northern Wisconsin: U.S. Geological Survey Open-File Report 81-577A, 31 p.

Geoterrex Ltd., With an introduction by Heran, W. D., 1981, Analog records from an Airorne Electromagnetic and Magnetic Survey of parts of the Upper Peninsula of Michigan and northern Wisconsin: U.S. Geological Survey Open-File Report 81-577B. (Microfiche only)

Kalliokoski, J. O. K., 1977, Uranium, thorium and potassium content of Precambrian rocks, Upper Peninsula of Michigan and northern Wisconsin: Bendix Field Engineering Corp., Grand Junction, Colo. (U.S. Energy Research and Development Admin.; GJBX 43 77).

Peters, W. C., 1978, Exploration and Mining Geology, Chap. 13, p. 377.

Saunders, D. F. and Potts, 1978, Manual for the Application of NURE 1974-1977 Aerial Gamma-Ray Spectrometer Data, Bendix Field Engineering Corp., U.S. Dept. of Energy Open-File Report 67BX-13(78).

U.S. Geological Survey, 1983, Stacked profiles of data from an airborne radiometric and magnetic survey of parts of the Upper Peninsula of Michigan and northern Wisconsin: U.S. Geological Survey Open File Report 83-195-B.

U.S. Geological Survey, 1982 Miscellaneous Investigation Series Map, Iron River CUSMAP Folio I-1360, A-N, 14 maps.

Selected References

Anderson, T. D., 1980, Magnetic Investigations of the Baraga County Diabase, Baraga County, Michigan: M. S. thesis, Michigan Technological University, Houghton.

Cannon, W. F., King, E. R., Hill, J. J., and Mory, P. C., 1980, Mineral Resources of the Sturgeon River Wilderness Study Area, Houghton and Baraga Counties, Michigan, U.S. Geological Survey Bulletin 1465.

Case, J. E., and Gair, J. E., 1965, Aeromagnetic Map of Parts of Marquette, Dickinson, Baraga, Alger, and Schoolcraft Counties, Michigan, and its Geologic Interpretation, U.S. Geological Survey Geophysical Investigation Map GP-467.

Johnson, C. A., 1977, Uranium and Thorium Occurrences in Precambrian Rocks, Upper Peninsula of Michigan, M. S. thesis, Michigan Technological University, Houghton.

Moshref, W. M., and Hinze, W. J., 1970, Geologic Interpretation of Aeromagnetic Data in Western Upper Peninsula of Michigan: Michigan Department of Natural Resources, Geological Survey, Report of Investigation 12.

Wier, K. L., Balsley, J. R., and Pratt, W. P., 1953, Aeromagnetic Survey of Part of Dickinson County, Michigan, With Preliminary Geologic Interpretation: U.S. Geological Survey Geophysical Investigation Map GP-115.

AIRBORNE RECONNAISSANCE GAMMA-RAY SPECTROMETRIC AND TOTAL FIELD MAGNETIC SURVEY IN THE UPPER PENINSULAR AREA OF MICHIGAN, AND IN NORTHERN WISCONSIN

Prepared By

HIGH LIFE HELICOPTERS, INC./QEB, INC.
Puyallup, Washington/Lakewood, Colorado

For The

UNITED STATES GEOLOGICAL SURVEY
Denver, Colorado

February, 1981

TABLE OF CONTENTS

VOLUME 1

FIGURES

INTRODUCTION

High Life Helicopters, Inc./QEB, Inc. have completed for the United States Geological Survey (USGS) an airborne reconnaissance gamma-ray spectrometric and total field magnetic survey over five areas in the Upper Peninsular of Michigan (Figure 1).

Data collection was done during September and October 1980 by High Life Helicopters, Inc. using two Aerospatiale Lama 315B helicopters equipped with gamma-ray spectrometers and magnetometers. Data reduction and analysis were done at QEB, Inc.'s data processing facility in Lakewood, Colorado.

The objective of the survey was a mineral evaluation and general appraisal of mineral exploration methods within the areas surveyed.

This report describes the equipment used, gamma-ray spectrometer calibration, survey methods, data reduction methods, data presentation and results.

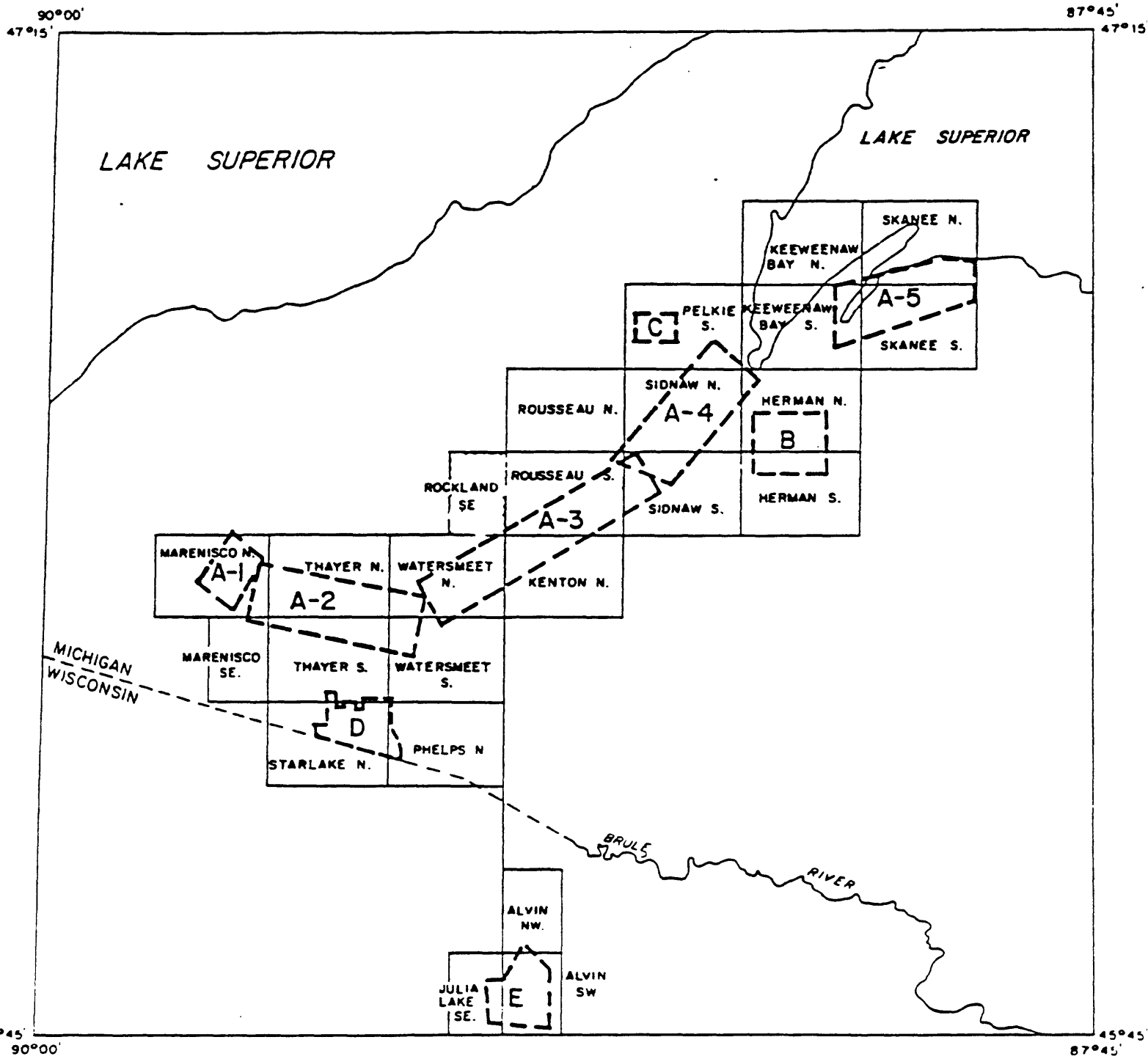

LOCATION MAP

SCALE: 1:1,000,000

Figure 1

SUMMARY

High Life Helicopters, Inc./QEB, Inc. have completed an airborne reconnaissance gamma-ray spectrometric and total field magnetic survey in five areas in the Upper Peninsular area of Michigan: Jacobsville (sub-areas A1-A5), Northern Cusmap (Area B), Limestone Mountain (Area C), Sylvania Wilderness (D), Wilderness (Area E). Two Aerospatiale Lama helicopters (U.S. Registry Nos. N49537, and N87638) equipped with gamma-ray spectrometers and proton precession magnetometers collected the data. The gamma-ray spectrometer in N49537 (System 1) had 2048 cubic inches of sodium iodide crystals in the downward-looking detector and 256 cubic inches of sodium iodide crystals in the upward-looking detector. The gamma-ray spectrometer in N87638 (System 2) had 2048 cubic inches of sodium iodide crystals in the downward-looking detector and 320 cubic inches in the upward-looking detector. The magnetometers in both aircraft were Geometrics Model G-803 proton precession magnetometers with a nominal sensitivity of 0.25 gammas. A total of 1373.5 line-miles of radiometric and magnetic data were collected in the five areas. Visual techniques were used in navigation, and flight path film was obtained for subsequent precise position determination.

Spectrometer data were corrected for aircraft and cosmic background, Compton scattering in the detector crystals, atmospheric radon, and altitude. Statistical methods were used to determine the statistical validity of the spectrometer data. The magnetometer data were corrected for the diurnal variations in the total field. The reduced spectrometer and magnetometer data were stored on magnetic tape with the formats shown in Appendix A.

Stacked profiles of the radiometric, magnetic, and ancillary data were prepared. Statistical criteria for radiometric anomalies were established, and statistical anomaly maps were prepared for each of the radiometric variables. Comparison of the radiometric maps were made to establish uranium anomalies. Contour maps of

the total magnetic field data were prepared, and an interpretation of the magnetic data made. The data from the profiles, the magnetic contour maps, and the uranium anomaly maps were used to prepare a combined magnetic interpretation and uranium anomaly maps, which was plotted on flight line maps prepared on a topographic base at a scale of 1:24,000. These interpretation maps accompany this report.

EQUIPMENT

AIRCRAFT

The aircraft used to carry the gamma-ray spectrometers, the magnetometers, and associated electronic equipment were Aerospatiale SA 315B Lama helicopters, U.S. Registration Nos. N49537 and N87638. The Lama is manufactured in France by Societe National Industrielle, and is designed to haul heavy loads in rugged terrain. It operates economically and safely under the most rigorous requirements, so is an ideal aircraft for gamma-ray spectrometer surveys, which must be conducted with heavy payloads, at low speed, and at low altitudes.

The Lama is powered by an 870 SHP Turbomeca Artouste IIIB turboshaft engine, fueled from a 151.3 U.S. gallon (573 liter) fuel tank mounted in the center section of the fuselage. The main rotor is driven through a planetary gear-box with provision for free wheel on autorotation. A take-off drive for the tail rotor is mounted at the lower end of the main gearbox, and a torque shaft connects the latter to a small gearbox that houses the pitch control mechanism, and on which the tail rotor is mounted. Cyclic and collective pitch are power-controlled. Rotors consist of a three-blade main rotor and an antitorque rotor. The main blades are all-metal, are of constant chord, have hydraulic drag-hinge dampers, and are mounted on articulated hinges.

The light metal framework cabin is glazed, but the center and rear of the fuselage behind the cabin have an open triangular framework. The cabin seats a pilot and one passenger side by side and three more passengers behind the pilot. The landing gear is made up of skids with removable wheels. Provision

is also made for pneumatic floats for operation on water, and for inflatable emergency flotation gear. The aircraft can carry crystal packs weighing up to 2,204 lbs. (1000 Kg.) mounted on external slings. The Lama is a versatile aircraft, which can be adapted for use in rescue operations, liason duties, training, agriculture, and aerial photography. External dimensions, performance, and weight specifications are listed below.

EXTERNAL DIMENSIONS

Main Rotor diameter	36' 1-3/4"
Tail Rotor diameter	6' 3-1/2"
Main Rotor Blade chord (constant)	13.8"
Length overall; both rotors turning	42' 4-3/4"
Length of fuselage	33' 8"
Height overall	10' 1-3/4"
Skid track	7' 9-3/4"

GENERAL PERFORMANCE SPECIFICATIONS
BASED ON SEA LEVEL STANDARD CONDITIONS

		Internal		External	
		Average	Maximum	Average	Maximum
At Gross Weight	lb	3,310	4,310	4,200	5,070
Empty Weight	lb	2,216	2,216	2,216	2,216
Useful Load	lb	1,094	2,084	1,984	2,854
Sling Load (Max)	lb	-	-	-	2,500
Cruise Speed	mph	118	-	55	75
Top Speed, Vne	mph	-	130	-	-
Useable Fuel US	gal	146	146	46	46
Service Ceiling	ft	(23,000)	17,000	18,000	10,800
HIGE Ceiling	ft	(23,000)	16,000	17,000	9,220
HOGE Ceiling	ft	(23,000)	15,170	16,100	5,000

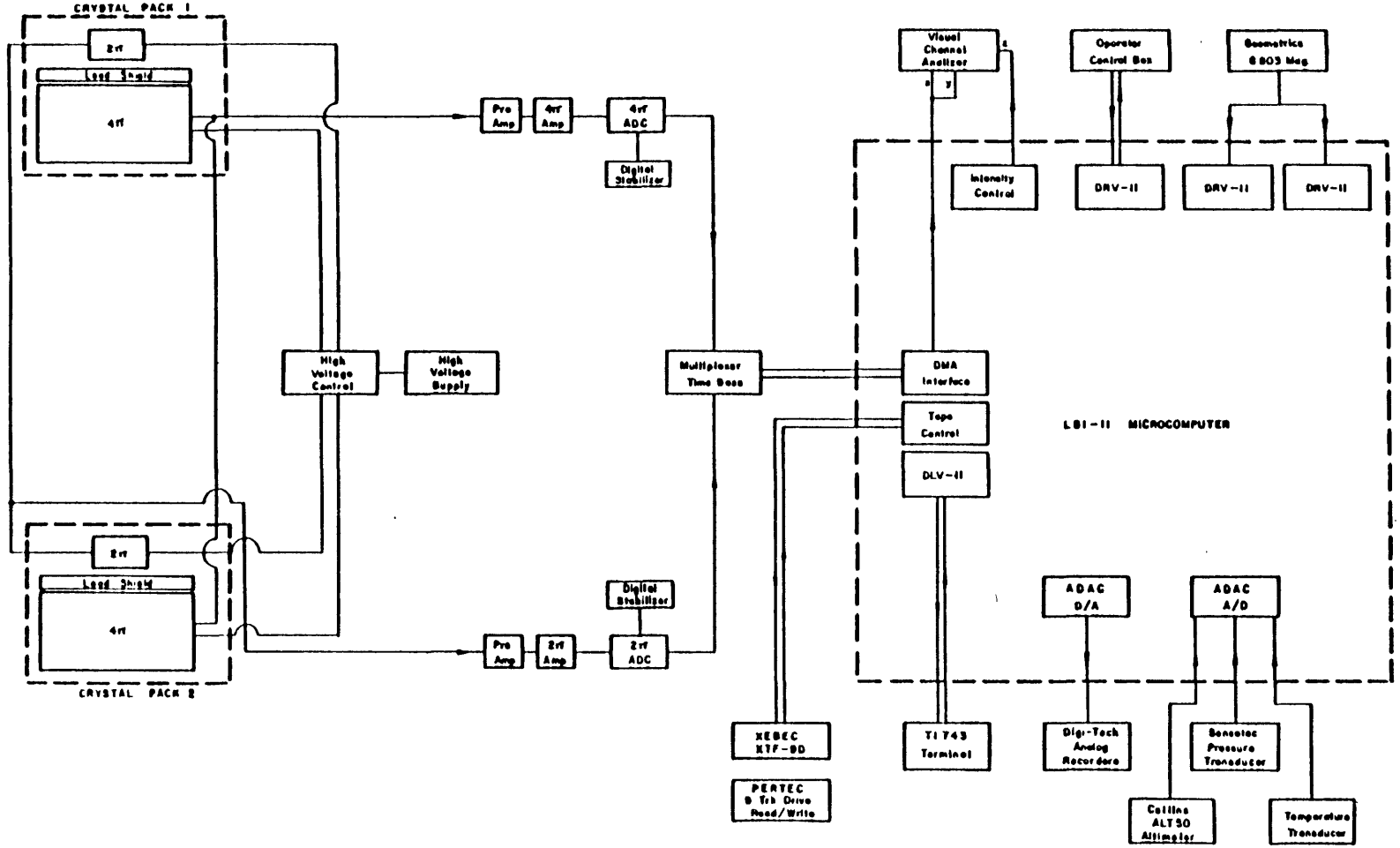

High Life Helicopters, Inc. / QEB Inc.

System Block Diagram

Lama Helicopter N 49537

FIGURE 2

WEIGHT SPECIFICATIONS FOR GEOPHYSICAL SURVEYS

	Weight (lbs)
LAMA empty weight	2216
Maximum useable fuel	900
Sensor Electronics	850
Pilot	160
Navigator	160
Total	4286

SENSORS

Two geophysical sensor systems with associated electronics were used in the survey: System #1 in Lama N49537 and System #2 in Lama N87638. A summary of each system is presented below, and schematic diagrams of each system are shown in Figures 2 and 3.

System #1 - Lama N49537 (Figure 2)

Geophysical Sensors

1) Crystal Gamma-Ray Detectors: Downward-looking, eight (8) sodium iodide crystals manufactured by Harshaw Chemical Co., Solon, Ohio. These are arranged in two packs, each containing four (4) crystals, mounted fore and aft on the under-side of the aircraft on bomb shackles fitted with a quick-release mechanism. Each crystal has a volume of 256 cubic inches for a total volume of 2048 cubic inches in the downward-looking detector.

2) Crystal Gamma-Ray Detectors: Upward-looking, one (1) sodium iodide crystal with a volume of 256 cubic inches mounted on top of the aft downward-looking crystal pack.

3) Towed-bird proton precession magnetometer, Geometrics Model G803, with a sensitivity of 0.25 gammas.

Ancillary Equipment

1) Radar Altimeter - Collins ALT-50.
2) Barometric Altimeter - Sensotec Pressure Transducer.
3) Recording Temperature Transducer.
4) Tracking Camera - Automax 35mm Framing Camera (Automax Industries, Woodland Hills, California).

Geophysical Console Equipment

1) A Geometrics G-714 Airborne Data Acquistion system is used to digitize and process all data from the sensors. The G-714 provides, along with its support equipment, analog to digital conversion, analog and digital gain stabilization, and formatting for the magnetic tape equipment.

2) Geometrics G-800 Gamma-Ray Spectrometer System.

3) Geometrics G-900 Sensor Interface and Power Supply.

4) Geometrics G-803 Magnetometer with 0125 gammas sensitivity.

Recording Equipment

1) Kennedy 9-track digital tape deck recording at 800 bpi. The system records:

   a) 512 channels of gamma-ray spectrometer data (256 down and 256 up),
   b) Total magnetic intensity,
   c) Fiducial number from data system and camera,
   d) Altitude from radar and barometric altimeters,
   e) Time (days, hours, minutes, seconds),
   f) Outside temperature,
   g) "Label" information - date, survey area, and flight number.

2) Geometrics GAR-6 channel chart recorder.

System #2 - Lama N87638 (Figure 3)

Geophysical Sensors

1) Geodata Model 9600 Airborne Radiometric System.

2) Crystal Detectors - consisting of ten (10) sodium iodide crystals manufactured by Harshaw Chemical Co., Solon, Ohio. These are arranged in two packs with each pack containing four (4) 256 cu. in. downward-looking crystals and one (1) 160 cu. in. upward-looking crystal. The packs are mounted on the underside of the aircraft on bomb-shackles fitted with a quick-release mechanism.

3) Magnetometer - Geometrics Model G-803 proton precession magnetometer with a 0.25 gamma sensitivity.

Ancillary Equipment

1) Radar Altimeter - Collins ALT-50.
2) Barometric Altimeter - Sensotec Pressure Transducer.
3) Recording Temperature Transducer.
4) Tracking Camera - Automax 35mm Framing Camera (Automax Industries, Woodland Hills, California.

Geophysical Console Equipment

1) LSI-II microcomputer (Digital Equipment Corporation) - basic system control.

2) Digital gain stabilizer, multiplexer, time base, high speed A to D and DMA Interface (Geodata International) to monitor and control count rates.

Recording Equipment

1) Pertec 9-track digital tape deck recording at 800 bpi. An Xebec Model XTF-90 tape controller is used to interface with the LSI-II. The system records:

   a) 512 channels of gamma-ray spectrometer data (256 up and 256 down).
   b) total magnetic intensity,
   c) fiducial number from data system and camera,
   d) altitude from radar and barometric altimeter,
   e) time (day, hours, minutes, seconds),
   f) outside temperature,
   g) "label" information - date, survey area, and flight number.

2) Digi-Tech analog recorder

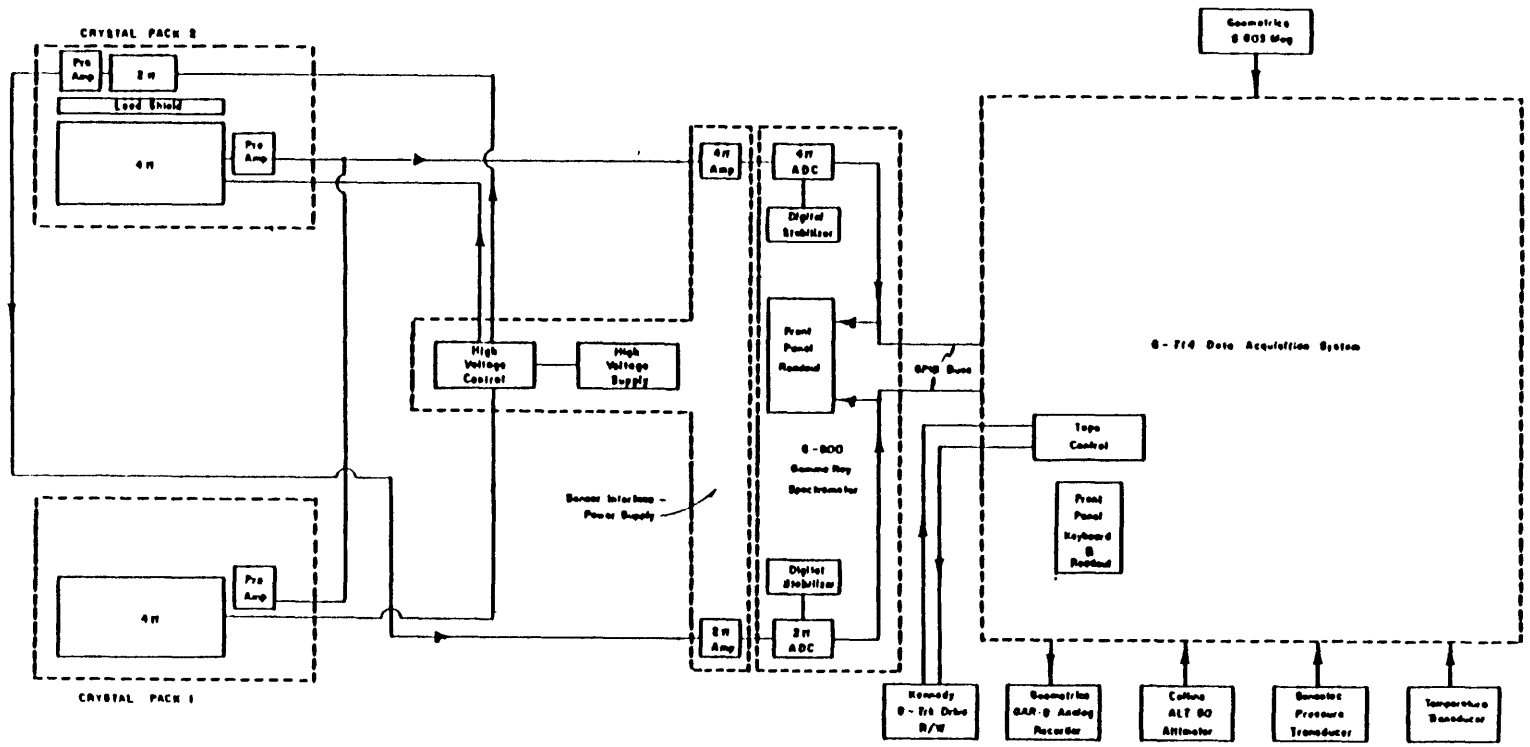

High Life Helicopters, Inc. / QEB Inc

System Block Diagram

Lama Helicopter

N 87638

DATA PROCESSING

QEB Inc. uses a Hewlett-Packard 1000 computer to process the geophysical data. The HP-1000 has a Fast Fortran Processor, 512K bytes of CPU memory, and 120 mega-bytes of on-line disc memory. Input/Output devices include three HP-7970B tape-drives, an HP-2648A graphics terminal, two HP-2621A CRT terminals, and an HP-2608A graphics printer.

Peripheral equipment used in the data processing includes:

1) A Calcomp 936 Drum Plotter
2) A Calcomp 915 Plotter Controller
3) A Talos BL648B Digitizer

The Calcomp Plotter can be driven either on-line by the HP-1000, or off-line by the Calcomp 915 Plotter Controller controlled from tapes generated by the HP-1000.

The Calcomp 915 Plotter Controller is a programmable device consisting of a central processing unit (CPU), a memory unit, a read-write magnetic tape cartridge unit, and a read-only magnetic tape unit (MTU). The 915 Plotter Controller can accomodate as many as five peripheral input-output devices on-line.

The MTU reads a data tape created by the HP-1000. The CPU and a system program read into memory from a tape cartridge, then convert the data on the tape into commands that drive an output device, e.g. the 936 Plotter.

The Talos BL648B Digitizer converts the coordinates of the physical position of pen or cursor on the activated digitizer surface into a digital output that can be entered through a remote terminal into the HP-1000 computer. The Talos BL648B has an active digitizing area of 48 X 36 inches.

SYSTEM CALIBRATION

COSMIC AND BACKGROUND

Background effects due to the natural radioactivity of the aircraft frame, geophysical equipment and other ancillary devices may be calculated from a series of high altitude sorties. To demonstrate this, consider the count rate at Energy E due to Compton scattering from a higher energy photon E'. For a constant elevation Z, we may write:

$$I(E,Z) = R(E';E,Z) + I_B(E) \qquad (1)$$

where:

$I(E,Z)$ is the count rate at energy E and altitude Z,

$R(E',E,Z)$ is the count rate at energy E and altitude Z due to a higher energy photon E',

$I_B(E)$ is the desired aircraft background (independent of Z).

For a given channel Ch, we may write for the high altitude test:

$$\int_{Ch} I(E,Z)dE = \int_{Ch}\int_{3MEV}^{6MEV} R(E';E,Z)dE\ dE' + \int_{Ch} I_B(E)dE \qquad (2)$$

where the double integral term on the hand side of (2) represents the cosmic contribution of the count rate measured in channel Ch. We must now specify the functional form for $R(E';E,Z)$ in order to solve for the cosmic and background effects. We make two assumptions regarding this function:

a) R is a function of the difference between the photon at energy E' and the lower energy level E,

$$R(E'-E,Z) = R'(E'-E,Z) \tag{3a}$$

b) R' can be separated into the product of two functions

$$R'(E'-E,Z) = P(E',Z)Q(E) \tag{3b}$$

Assumption (3a) postulates that the effect at lower energies depends only upon the energy <u>difference</u> between E' and E. A suggested functional form for R' is exponential, i.e:

$$R'(E'-E,Z) = f(Z)\ \exp\ (C(E'-E) \tag{4}$$

The form (4) seems to be born out experimentally. Whatever the relative merits of assumption (a), assumption (b) is critical to our analysis. We assume that R' can be separated into the product of a function of E' and Z with a function only of E. This assumption will allow us to treat the cosmic correction and background as a linear effect.

Substituting equation (3b) into (2), we find:

$$\int_{Ch} I(E,Z)dE = \int_{3MEV}^{6MEV} P(E'Z)dE' \int_{Ch} Q(E)dE + \int_{Ch} I_B(E)dE \tag{5}$$

Equation (5) can be written in the functional form for any channel:

$$Y = A * X + B \tag{6}$$

where

$Y = \int_{Ch} I(E,Z)dE$ Is the measured count rate at altitude

Z in channel Ch.

$X = \int_{3MEV}^{6MEV} P(E'Z)dE'$ is the measured cosmic count rate at altitude Z.

$A = \int_{Ch} Q(E)dE$ is a dimensionless quantity which weights the cosmic count rate to indicate the integral count rate within a channel Ch due to cosmic energies. A is also referred to as the cosmic correction ratio

$B = \int_{Ch} I_B(E)dE$ is the background in counts per second.

The quantities A and B are determined by a least squares analysis of channel data over the suite of five flight altitudes.

SYSTEMS CONSTANTS

System constants were determined at the DOE Walker Field test pads and at the Lake Mead Test Range. The test areas at these sites contain known concentrations of potassium, uranium, and thorium. The concentrations of elements in the five pads at Walker Field are shown in the table below:

ELEMENT CONCENTRATION IN THE
WALKER FIELD PADS

Pad		K	U	Th
1.	Background/Matrix	1.45%	2.19 ppm	6.26 ppm
2.	(K)	5.14%	5.09 ppm	8.48 ppm
3.	(U)	2.03%	30.29 ppm	9.19 ppm
4.	(Th)	2.10%	5.14 ppm	45.33 ppm
5.	Mixed	4.11%	20.39 ppm	17.52 ppm

Full spectral data were measured and digitally recorded above each of the calibration pads at Walker Field. Data were collected over each pad during a five minute interval. A sample rate of one full scan per second - 256 channels for the down-crystal, and 256 channels for the up-crystal - gave a total of 300 spectral measurements per calibration pad. Since the calibration measurements were taken over a comparatively short time period, it was assumed that the individual pad measurements contain not only the effects of the pad itself; but the aircraft background - constant for a particular aircraft; cosmic background - constant over the measurement period; and the local background Bi-air etc. When the Background/Matrix pad count rate values were subtracted from the values obtained over the other pads; the aircraft, the cosmic, and the local backgrounds were eliminated. The pad concentrations were similarly modified by subtracting the Background/Matrix concentration from each of the remaining four pads to give the differential element concentration.

DIFFERENTIAL ELEMENT CONCENTRATIONS
WALKER FIELD PADS

	Pad	K	U	Th
K - Matrix	2-1	3.69%	2.90 ppm	2.22 ppm
U - Matrix	3-1	0.58%	28.10 ppm	2.93 ppm
Th - Matrix	4-1	0.56%	2.95 ppm	39.07 ppm
Mixed - Matrix	5-1	2.66%	18.20 ppm	11.26 ppm

The count rate over pads 2 through 5 could then be related directly to the differential concentrations of the elements in these pads.

Sensitivity Coefficients - Theory

It can be demonstrated that the observed count rate of a spectrometric system is a function not only of the mean ground level abundance of radioactive elements, but also of other parameters such as crystal geometry, flight altitude, equivalent optical path length, etc.

Consider the response of an ideal spectrometer (one with infinitely precise resolving power) to gamma-ray excitation from a radioactive ground source.

For a given monochromatic energy E_0:

$$I(E_0) = \varepsilon \int_s \frac{I' A e^{-\mu R}}{R^2} dS \qquad (1)$$

where

$I(E_0)$ Is the theoretical count rate at energy E_0.

ε Is the photo-detector efficiency at energy E_0.

A Is the solid angle response of the spectrometer system.

μ Is the attentuation constant of the medium through which the photon of energy E_0 passes.

R Is the distance from an elemental ground surface of area dS to the photo-detector.

I' Is the surface count rate which is propor-

tional to the ground level abundance of radioactive elements at Energy E_0.

The relative simplicity of (1) is deceiving, since complicated interactions such as Compton scatter in the ground and in the air are assumed to be approximated by the simple exponential attenuation coefficient μ. A further complication is that any spectrometer system has less than ideal resolving power. Thus, the more or less monochromatic energies from ground sources are "smeared" over a broad range of energy levels. This "smearing" is due to photon-crystal interactions (Compton scatter), amplifier drift, thermal effects, etc. The observed spectra can now be written as:

$$I'(E_0;E) = I(E_0)R(E_0;E) \qquad (2)$$

where

$I'(E_0;E)$ Is the observed count rate at energy E due to monochromatic source at energy E_0.

$I(E_0)$ Is the intensity of the monochromatic emitter.

$R(E_0;E)$ Is the crystal response function due to a monochromatic input photon.

Sensitivity Coefficients Applicable to the Walker Field Test Pads

Let us now relate this theoretical discussion to the Walker Field Test Facility measurement assuming that the air attenuation constant was invariant over the measurement period.

and that the pad geometries were similar, then from equation (1) we may write:

$$I(E_o) = C(E_o)\rho(E_o) \qquad (3)$$

where

$C(E_o)$ Is a proportionality constant for a given energy E_o.

$\rho(E_o)$ Is the ground level concentration of radioactive elements of energy E_o.

Let us consider the expected count rates from the Walker Field pads.

From Equations (2) and (3), we may write:

$$I'_j(E_k,E_u,E_T;E) = C(E_k)R(E_k;E)\rho(E_k,j) + C(E_u)R(E_u;E)\rho(E_u,j)$$

$$C(E_T)R(E_T;E)\rho(E_T,j) + B(E) \qquad (4)$$

where

E_k = 1.46 MeV (K_{40} Photopeak),

E_u = 1.76 MeV (Bi_{214} Photopeak),

E_T = 2.62 MeV (Tl_{208} Photopeak),

$\rho(E_k,j)$ = Concentration of K_{40} in the j pad,

$\rho(E_u,j)$ = Concentration of U_{238} in the j pad,

$\rho(E_T,j)$ = Concentration of Th_{232} in the j pad,

$B(E)$ = Background Count rate

$I'(E_k,E_u,E_T;E)$ = Observed Count Rate at E Due to concentrations of K_{40}, U_{238}, and Th_{232}.

If we let

${}^{k}I'_{j}$ = Count Rate of K channel measured on pad j.

${}^{u}I'_{j}$ = Count Rate of U channel measured on pad j.

${}^{T}I'_{j}$ = Count Rate of Th channel measured on pad j.

Then we may write a set of 3 matrix equations for each channel measurement

K CHANNEL

$$\begin{pmatrix} {}^{k}I'_{2} \\ {}^{k}I'_{3} \\ {}^{k}I'_{4} \\ {}^{k}I'_{5} \end{pmatrix} = \begin{pmatrix} \rho(E_k,2) & \rho(E_u,2) & \rho(E_T,2) \\ \rho(E_k,3) & \rho(E_u,3) & \rho(E_T,3) \\ \rho(E_k,4) & \rho(E_u,4) & \rho(E_T,4) \\ \rho(E_k,5) & \rho(E_u,5) & \rho(E_T,5) \end{pmatrix} \begin{pmatrix} {}^{k}s_{k} \\ {}^{k}s_{u} \\ {}^{k}s_{t} \end{pmatrix} + B_k \quad (5a)$$

U CHANNEL

$$\begin{pmatrix} {}^{u}I'_{2} \end{pmatrix} \qquad \begin{pmatrix} \rho(E_k,2) & \rho(E_u,2) & \rho(E_T,2) \end{pmatrix}$$

$$\begin{pmatrix} {}^{U}I'_3 \\ {}^{U}I'_4 \\ {}^{U}I'_5 \end{pmatrix} = \begin{pmatrix} \rho(E_k,3) & \rho(E_u,3) & \rho(E_T,3) \\ \rho(E_k,4) & \rho(E_u,4) & \rho(E_T,4) \\ \rho(E_k,5) & \rho(E_u,5) & \rho(E_T,5) \end{pmatrix} \begin{pmatrix} {}^{U}S_k \\ {}^{U}S_u \\ {}^{U}S_t \end{pmatrix} + B_u \quad (5b$$

Th CHANNEL

$$\begin{pmatrix} {}^{T}I'_2 \\ {}^{T}I'_3 \\ {}^{T}I'_4 \\ {}^{T}I'_5 \end{pmatrix} = \begin{pmatrix} \rho(E_k,2) & \rho(E_u,2) & \rho(E_T,2) \\ \rho(E_k,3) & \rho(E_u,3) & \rho(E_T,3) \\ \rho(E_k,4) & \rho(E_u,4) & \rho(E_T,4) \\ \rho(E_k,5) & \rho(E_u,5) & \rho(E_T,5) \end{pmatrix} \begin{pmatrix} {}^{T}S_k \\ {}^{T}S_u \\ {}^{T}S_T \end{pmatrix} + B_T \quad (5c$$

where

$$ {}^{L}S_M = \int_L C(E_M) R(E_M;E) dE $$

$$ L,M = K,U,T \quad (6) $$

We can interpret (6) as the weighted sum of the crystal response in channel L, due to an elemental input photon in channel M. Clearly, if L is of higher energy than M, we would expect a value of (6) to be nearly zero. The units of ${}^{L}S_M$ are counts/sec/elemental concentration.

The set of matrix equations (5a) through (5c) represents a set of 12 equations with 9 unknown variables ${}^{L}S_M$. To solve these equations the count rates measured on pads 2 through 5 were fit in a least square sense. The background values B_k, B_u, B_{Th}, were estimated from averaged measurements from pad 1.

The differential concentrations, as supplied by Bendix Field Engineering Corporation, are tabulated on page 14. Only data for the down crystals were used in the least squares analysis.

For each pad measurement, a matrix equation may be written relating the observed count rate to the elemental concentration by the least squares sensitivity matrix. Thus, from (5a), (5b), and (5c):

$$\begin{pmatrix} {}^{k}I'_{j} \\ {}^{u}I'_{j} \\ {}^{T}I'_{j} \end{pmatrix} = S \cdot \begin{pmatrix} \rho(E_k;j) \\ \rho(E_u;j) \\ \rho(E_T;j) \end{pmatrix} \begin{pmatrix} B_k \\ B_u \\ B_T \end{pmatrix} \tag{7a}$$

where

$$S = \begin{pmatrix} {}^{k}s_{k} & {}^{k}s_{u} & {}^{k}s_{T} \\ {}^{u}s_{k} & {}^{u}s_{u} & {}^{u}s_{T} \\ {}^{T}s_{k} & {}^{T}s_{u} & {}^{T}s_{T} \end{pmatrix} \tag{7b}$$

Upon inverting (7a), the elemental concentrations may be solved for in terms of the observed count rates.

$$\begin{aligned} \rho(E_k,j) &= S_3 \left(({}^{k}I'_{j} - B_k) - {}^{k}\phi_u ({}^{u}I'_{j} - B_u) - {}^{k}\phi_T ({}^{T}I'_{j} - B_T) \right) \\ &= S_3 \, {}^{k}I_{corr} \end{aligned} \tag{8a}$$

$$\rho(E_u,j) = S_2 \left(({}^{u}I'_{j} - B_u) - {}^{u}\phi_T ({}^{T}I'_{j} - B_T) - {}^{u}\phi_k ({}^{k}I'_{j} - B_k) \right)$$

$$= S_2 {}^{u}I_{corr} \quad (8b)$$

$$\rho(E_T, j) = S_1 \left(({}^{T}I'_j - B_T) - {}^{T}\phi_k ({}^{k}I'_j - B_k) - {}^{T}\phi_u ({}^{u}I'_j - B_u) \right)$$

$$= S_1 {}^{T}I_{corr} \quad (8c)$$

Where ${}^{k}I_{corr}$ ${}^{u}I_{corr}$ and ${}^{T}I_{corr}$ are the Compton and background corrected count rates for k, u, and T respectively; S_3, S_2, and S_1 are the inverse sensitivities of the crystal packs relative to k, u, and T, respectively. The quantities ${}^{M}\phi_L$ are the full stripping Compton coefficients (dimensionless) which relate the effect in channel M of a photon in channel L.

Both Compton coefficients and sensitivities are determined from a least squares regression on count rates measured on pads 2 through 5. Pad 1 is used as a reference pad to establish the background count rates.

ATMOSPHERIC RADON CORRECTION

For notational purposes, we designate the count rates measured at Lake Mead in the following form:

$$\text{Count Rate} = {}^{(U.D.)}(K,U,T,C)'_{(L,W)}$$

Where K, U, and T refer to the Potassium, Bismuth, and Thallium channels respectively.

The superscripts (U.D) refer to the up (2π) and down (4π) crystals respectively. The subscripts (L,W) refer to count rates measured over land and water respectively. The prime (') indicates that the count data are corrected for background and stripped. The raw data are unprimed.

For example, ${}^{u}U_{W}$ refer to the raw data in the Bismuth channel

measured by the 2π crystal over water.

Consider the four experimental situations encountered at Lake Mead.

WATER

$$^{D}U_{W} = Bi_{A} + {}^{D}B_{u} \longrightarrow + {}^{u}\phi_{k}\,(^{D}K_{w} - {}^{D}B_{k}) + {}^{u}\phi_{T}\,(^{D}T_{W} - {}^{D}B_{T}) +$$

$$\text{Cosmic } 4\pi \qquad (2a)$$

$$^{U}U_{W} = \phi_{B}\, Bi_{A} + {}^{U}B_{u} + \text{Cosmic } 2\pi$$

LAND

$$^{D}U_{L} = Bi_{A} + {}^{D}B_{u} + U_{G} + {}^{u}\phi_{k}\,(^{D}K_{L} - {}^{D}B_{k}) + {}^{u}\phi_{T}\,(^{D}T_{L} - {}^{D}B_{T}) +$$

$$\text{Cosmic } 4\pi \qquad (3a)$$

$$^{U}U_{L} = \phi_{B}Bi_{A} + {}^{U}B_{u} \longrightarrow + B_{o}\,(Z)\,{}^{D}U'_{L} + C_{o}\,{}^{D}T'_{L} + \text{Cosmic } 2\pi$$

(3b)

Where Bi_A is the count rate due to atmospheric bismuth within the channel. It is assumed that the Bi_A level is invariant over land or water (perfect atmospheric mixing). Bi_A can; however, vary with survey altitude.

$^{(U,D)}B_{(k,u,T)}$ are the up and down backgrounds (established by the high altitude tests).

Cosmic 2π (4π) are the cosmic corrections for the Bi channel.

U_G is the count rate in the Bi channel due to ground sources,

$B_o(Z), C_o$ are the counts observed in the upward-looking Bi channel per downward-looking count in "stripped" U and T respectively,

ϕ_B is the fraction of Bi_A detected by the 2π crystals with respect to the 4π crystals.

B_o and C_o are the fraction of U_G detected by the 2π crystals, with respect to the 4π crystals.

To determine Bi_A over land, we first calculated ϕ_B from the over water data. From equations (2a) and (2b) we have:

$$\phi_B = \frac{U_{U_W} - U_{B_U} - \text{Cosmic } 2\pi}{D_{U_W} - D_{B_U} - \text{Cosmic } 2\pi} \qquad (4)$$

A linear least squares fit established the altitude of ϕ_B.

Similarly, we can determine the altitude dependence of B_o and C_o.

The value of $B_o(0)$ and $C_o(0)$ were established at the Walker Field Test Facility.

With B_o and C_o estimated, the air effect on the bismuth channel may be written:

$$Bi_A = \frac{U_{up} - B_o\,(Z)\,U'_L - C_o T_L'}{\phi_B\,(Z) - B_o\,(Z)} \qquad (5)$$

Where:

U_{up} is the count rate from the upward-looking detector corrected for cosmic and background effects.

$B_o(Z), C_o$ are the counts observed in the upward-looking Bi channel per downward-looking in "stripped" U and T respectively.

$\phi_B(Z)$ is the 4π to 2π geometric ratio.

U_L' is the Compton Scatter corrected Bi count rate (4π detector).

T_L' is the Compton Scatter corrected Tl count rate.

DATA COLLECTION

PRODUCTION SUMMARY

A total of 1373 line-miles of spectrometric and magnetic data was collected in the five areas flown in this project. Table 1 summarizes the flight information for each area.

TABLE 1

AREA	DATE COMMENCED	DATE COMPLETED	LINE-MILES	AIRCRAFT
A1 Jacobsville	10/21/80	10/21/80	81.50	N87638
A2 "	10/15/80	10/21/80	241.50	N87638
A3 "	10/09/80	10/14/80	390.75	N87638
A4 "	10/09/80	10/08/80	210.25	N87638
A5 "	10/08/80	10/08/80	188.50	N87638
B Northern Cusmap	10/09/80	10/09/80	84.00	N87638
C Limestone Mt.	10/08/80	10/08/80	30.00	N87638
D Sylvania Wilderness	09/11/80	09/11/80	75.00	N49537
E Wilderness Area	09/24/80	09/24/80	72.00	N49537

In the Jacobsville area (A1-5) traverse lines were flown at half-mile spacing perpendicular to the long axis of each sub-area; two tie lines were flown, one on each side of the major geologic unconformity, and parallel to the long axis of each sub-area. In the remaining four areas, flight lines were flown NS at half-mile spacing, and tie lines were flown perpendicular to the flight lines (see flight line maps accompanying report).

FLIGHT PROCEDURES

Operating Parameters - System #1 - N49537

1. Data sampling rates of the system elements are shown below:

SYSTEM ELEMENT	SAMPLE RATE
8 Downward-looking crystals (Total volume of 2048 cu. ins).	1.0 second (256 channels and cosmic)
2 Upward-looking crystals (Total volume of 320 cu. ins.)	1.0 second (256 channels and cosmic)
Live Time (4π) system	1.0 second (Binary output)
Live Time (2π) system	10.0 second (Binary output)
Geometrics G803 Magnetometer (0.25 gamma sensitivity)	1.0 second (BCD output)
Ancillary Sensors	
Collins ALT-50 Altimeter Sensotec Pressure Transducer	
Temperature Transducer	
Radar Altimeter	
Clock (hours, minutes, seconds)	1.0 second (Binary output)
Automax 35mm framing camera	3.0 seconds

2. At the end of a line, the summed spectra for both the 4π system and the 2π system were written to magnetic tape. The purpose was to ensure channel resolution and photopeak stability in subsequent processing.

3. Lama nominal ground speed was 90 mph. With a downard crystal volume of 2048 cu. ins., the ratio V/v = 22.76 cu. ins./mph.

This average speed was not exceeded except when dictated for aircraft safety.

Operating Parameters - System #2 - N87638

1. Data sampling rates of the system elements are displayed below:

SAMPLE ELEMENT	SAMPLE RATE
8 Downward-looking crystals (Total volume of 2048 cu. ins.)	1.0 second (256 channels and cosmic)
1 Upward-looking crystal - shielded (Total volume of 256 cu. ins.)	10.0 seconds (256 channels and cosmic)
Live Time (4π) system	1.0 second (Binary output)
Live Time (2π) system	10.0 seconds (Binary output)
Geometrics G-803 Magnetometer	1.0 second (BCD output)
Ancillary sensors	
Collins ALT-50 Altimeter -Senstec Pressure Transducer	
Temperature Transducer	
Radar Altimeter	
Clock (hours, minutes, seconds)	1.0 second (Binary output)
Automax 35mm framing camera	3.0 seconds

2. At the end of a line, the summed spectra for both the 4π

system and the 2π system were written to magnetic tape. The purpose was to ensure channel resolution and photopeak stability in subsequent processing.

3. Lama nominal ground speed was 90 mph. With a downward crystal volume of 2048 cu. ins., the ratio V/v = 22.8 cu. ins./mph. This nominal speed was not exceeded except when dictated by aircraft safety.

DAILY SYSTEM CALIBRATION

System #1 - Lama N49537

Pre-flight Checks

a) Cesium sources were positioned at the same point on both the 4π and 2π detector crystals each day to peak each photomultiplier tube. The oscilloscope display and LSI-II microcomputer output indicated the optimum peak setting.

b) The full cesium spectrum was displayed on the cathode-ray tube (CRT) for both upward-looking and downward-looking crystals to calculate the cesium resolution.

c) Thorium sources were used to verify the high energy end of the spectrum for the upward-looking and downward-looking crystals. The output is displayed on the CRT or the LSI-II.

d) The full thorium spectrum for the downward-looking crystals was displayed to verify the location of the K40 and the thorium photopeaks.

In-flight Checks

a) Each day, prior to production flying, a test line approximately

5 miles long was flown at the planned survey altitude. Data from the test line were examined to ensure ± 20% repeatability of the total counts.

b) During production flying, the visual display units were carefully monitored to detect changes in data quality.

System #2 - Lama N87638

Pre-flight Checks

a) Cesium sources were positioned at the same point on both the 4π and 2π detector crystals each day to peak each photomultiplier tube. The G-800 has a digital split window detector to indicate optimal peak setting. Output from this detector is displayed on the G-800 front panel when operating in "calibration mode".

b) Thorium sources were used to verify the high energy end of the spectrum for the upward-looking and downward-looking crystals. The output is displayed on the G-800 front panel.

c) The full thorium spectrum for the downward looking crystals was displayed to verify the location of the K40 and the Th238 photopeaks.

In-flight Checks

a) Each day, prior to production flying, a test line approximately 5 miles long was flown at the planned altitude. Data from the test line were examined to verigy ± 20% repeatability of the total count.

Post-flight Checks

a) Pre-flights checks were repeated to ensure that no malfunction in the data system occurred during the data collection.

FLIGHT PATH RECOVERY

Aircraft track was established by visual in-flight identification of prominent ground features by the operator. At the end of each production flight, all mislocations were adjusted by correlating the 35mm photos with USGS topographic map sheets. Final posting of flight track pick-points was done on 1:24,000 scale topographic map sheets.

DATA PROCESSING

PRE-PROCESSING

By "pre-processing", we refer to those procedures that are applied to the field data and flight line locations to prepare them for final processing, merging and output. Steps in this "pre-processing" stage included field data tape editing and compacting, flight line location verification, and generation of preliminary data reports. The reader is referred to the data processing flow chart, Figure 3, which accompanies this report, and which illustrates the steps described below.

Field Tape Compacting and Editing

A check of the field data tapes by computer is necessary to verify data collection and recording quality. The summed spectral data for both 4π and 2π crystals were first read from a series of merged field tapes. The centroids of channel photopeaks for each flight line were next calculated from these data, and a linear equation that relates the photo energy, in MeV, to the channel number was derived from the centroid calculation is of the form:

$$E = E(0) = dE/dch \times ch$$

Where E(0) is the apparent energy at channel zero, and ch is the channel number (0-255). This procedure was not applied if the survey line was too short (less than 10 minutes duration) to establish adequately smooth summed spectral data for photopeak calculations. Next the summed or "stacked" spectral data were used to calculate the resolution for k,u,Th photopeaks. Both photopeak linearity and resolution were used to establish the acceptability of the spectrometer data.

Next, the data within each flight line were checked for correct one (1) second and ten (10) second scan lengths. Erroneous scan lengths were flagged, and the spectral data for the erroneous scans were not used in the subsequent data analysis. In addition to these editing steps, the ancillary data (altimeter, pressure, and temperature) were computed from the transducer analogue voltage output. The data from each scan were used to extract one second channel window data fields, and these data fields were corrected for system "dead time". At the end of this stage of the data processing, two computer tapes were written (items 3 and 4 of Figure 3). Item 3 is a partially written RAW SPECTRAL TAPE (see Appendix A) containing all of the required data entries exclusive of the location information. Item 4 is a tape written in interval binary code. This tape contains all of the required entries for further processing. Full spectral data were not written on this tape, as these are contained on the partial RAW SPECTRAL TAPE.

In producing item 4, a series of computer generated histograms was produced for each survey line. Typically, these histograms summarize data recorded on the k, u, and Th channels (4π and 2π), together with ancillary data (altimeter, pressure, and temperature).

Editing was next performed on the binary tape. Further checking consisted of rereading (with unnecessary flight data removed); and searching for and removing unrealistic gradients, transients, spikes, etc. The acceptability of questionable data segments was reviewed and corrections performed. The result of this procedure was an edited tape, which has "clean" data available for step 5 of the data processing (Figure 3).

Flight Line Recovery

Determining actual flight-line location is a crucial task in the data processing. It is accomplished primarily by using photographs taken in flight. After the flight film is developed, a photo interpreter correlates the photo-data with the flight navigator's visual location picks on the NTMS map sheets. Actual aircraft locations were determined from the flight films and transferred to a base map with the fiducial numbers of the corresponding photographs. Once data transfer to the base map was complete, fiducial numbers and locations along each flight line were digitized, and an automated computer routine checked the consistency of these data. This was done by calculating the average distance between fiducials, and establishing that this distance was approximately constant along a given flight line. After computer verification, map coordinates for each photo pick point and the beginning and ending points of each flight line were calculated and a computer plot of these points made and checked against the field plot. Any discrepancies were noted, and the misplaced pick points relocated from the flight film. The procedure was repeated until consistency was achieved.

Once the flight line data was verified, a mylar transparency of the flight lines was prepared on the Cal Comp 915 at a scale of 1:250,000. This transparency was then overlain on the geologic base map and each map unit digitized so that each sample fell within a single unit.

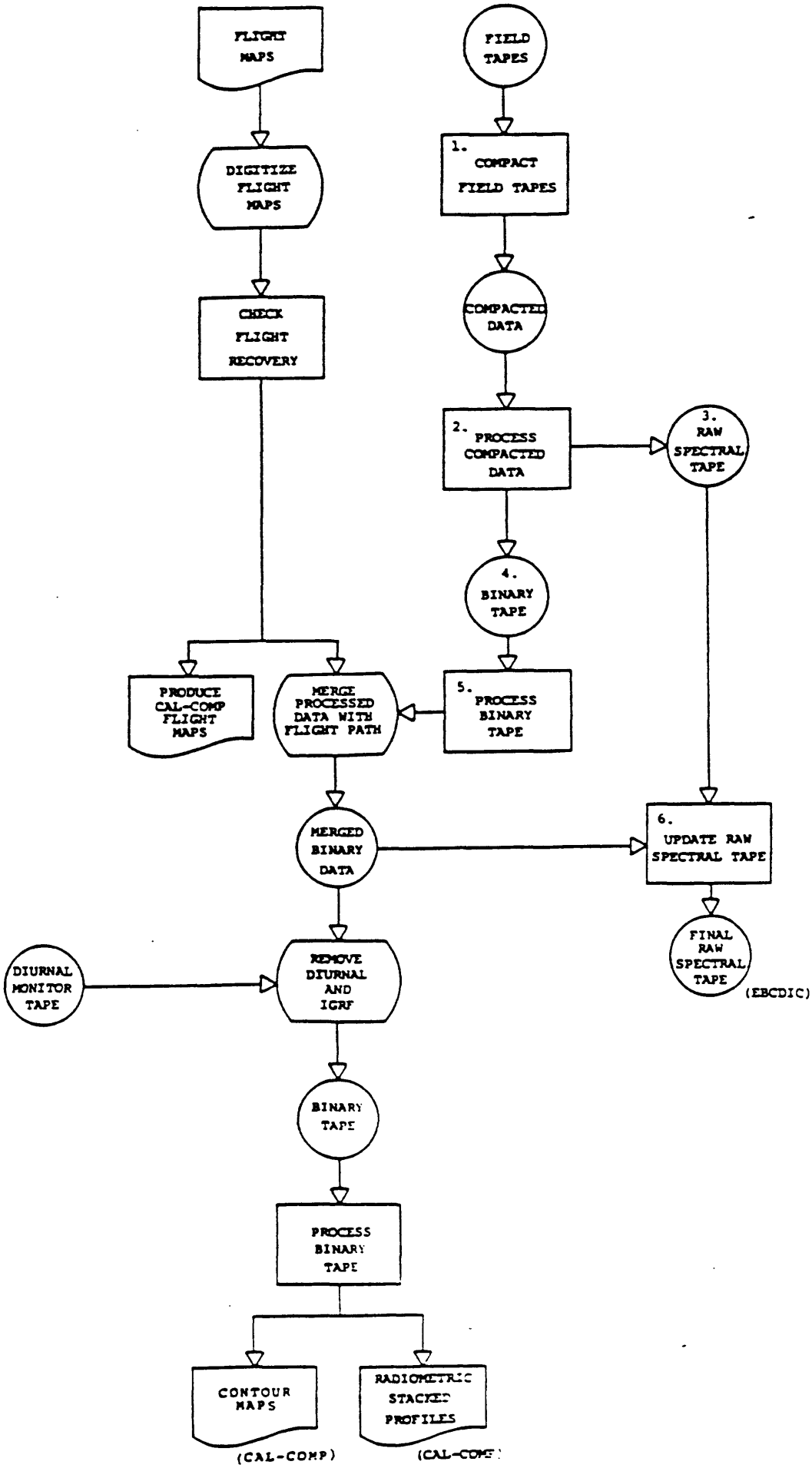
FLIGHT MAPS
FIELD TAPES
DIGITIZE FLIGHT MAPS
1. COMPACT FIELD TAPES
CHECK FLIGHT RECOVERY
COMPACTED DATA
2. PROCESS COMPACTED DATA
3. RAW SPECTRAL TAPE
4. BINARY TAPE
PRODUCE CAL-COMP FLIGHT MAPS
MERGE PROCESSED DATA WITH FLIGHT PATH
5. PROCESS BINARY TAPE
MERGED BINARY DATA
6. UPDATE RAW SPECTRAL TAPE
FINAL RAW SPECTRAL TAPE
(EBCDIC)
DIURNAL MONITOR TAPE
REMOVE DIURNAL AND IGRF
BINARY TAPE
PROCESS BINARY TAPE
CONTOUR MAPS
(CAL-COMP)
RADIOMETRIC STACKED PROFILES
(CAL-COMP)

Figure 4

$\phi_B(Z_{STP})$ = 4π to 2π geometric ratio (height dependent).

$B_o(Z_{STP})$ = 4π to 2π bismuth coupling factor.

C_o = 4π to 2π thallium coupling factor (constant).

Values for these factors were established at the Lake Mead Dynamic Test Range and the Walker Field Test Facility:

$B_o(Z)$ = 0.04254 EXP(-.0022973*Z(STP)) - #N49537

= 0.034287 EXP(-.000013515*Z(STP)) - #N87638

C_o = 0.01887196 - #N49537

= 0.01436084 - #N87638

$\phi_B(Z)$ = 0.2144653 - 0.00002659*Z(STP)) - #N49537

$\phi_B(Z)$ = 0.2916494 - 0.00002659 *Z(STP)) - #N87638

4. Altitude Correction

The altitude attenuation coefficients used in the correction of the data are listed below:

	N49537	N87638	
μ_{TC} =	-0.00216583	-0.0022202/ft.	
μ_K =	-0.00271859	-0.00285991/ft.	
μ_U =	-0.00256281		(least squares fit)
μ_U =	-0.00217342	-0.00267851/ft.	(interpolated value)

μ_T = -0.00208235 -0.00223058/ft.

These coefficients are employed to reduce the measured count rate at any elevation to 400 feet (at STP of 0°C - 760 mm. Hg). The reduction formula is given by:

$$\text{COUNTS NORMALIZED} = \text{COUNTS MEASURED} * \text{EXP}\ (+\mu_i * (Z_{STP} - 400))$$

$$Z_{STP} = Z_{MEAS} * \frac{P * 273.15}{760 * (273.15 + T)}$$

where:

μ_i is the channel altitude attenuation coefficient

P is the measured atmospheric pressure (mm. of Hg)

Z_{MEAS} is the radar altimeter altitude

T is the temperature is degrees Celsius

The reduction fo STP is necessary to correct for air density change along the ground-detector optical path.

5. Statistical Adequacy Criteria

To determine the statistical adequacy of raw count data R_j, subject to a subtracted correction term C_j, a number of assumptions are required concerning the statistical properties of both R_j and C_j. Further, the statistical effects of filtering (smoothing) R_j must be taken into account.

We assume, at any data point j, that R_j and C_j are both random variables on the same sample space. Further, we assume that

RADIOMETRIC DATA PROCESSING

The "cleaned" data require a number of corrections and statistical evaluation before data plots and statistical summaries can be produced. These are done in step 5 (Figure 3), and include:

1. Aircraft and cosmic background correction,
2. Compton Stripping,
3. Atmospheric radon correction,
4. Altitude correction,
5. Statistical adequacy criteria.

1. Aircraft and Cosmic Background Correction

Aircraft background and cosmic correction ratios for the two Lama helicopters over the channel windows are listed below:

AIRCRAFT AND COSMIC BACKGROUND

CHANNEL WINDOW	AIRCRAFT BACKGROUND COUNTS/SEC.		COSMIC CORRECTION RATIO (DIMENSIONLESS)	
	#N49537	#N87638	#N49537	#N87638
K-40 (4π)	6.02	20.27	0.2092	0.1033
Bi-214 (4π)	2.52	7.60	0.1825	0.0794
Tl-208 (4π)	2.37	2.45	0.2176	0.1066
TOTAL COUNT	64.68	133.94	3.4579	1.7186
Bi-214 (2π)	0.62	.60	0.2143	0.1102

2. Compton Stripping

Compton Scattering corrections to the 4π data were made using the following stripping coefficients:

	#N49 537	#N87638
k_{ϕ_u}	= 0.799243	= 0.819311
$k_{\phi_{Th}}$	= 0.142307	= 0.162482
$u_{\phi_{Th}}$	= 0.324194	= 0.295832
u_{ϕ_k}	= 0.017223	= 0.0
Th_{ϕ_u}	= 0.094613	= 0.081863
Th_{ϕ_k}	= 0.0	= 0.0

3. Atmospheric Radon Correction

The Bi-air (Radon) contribution to the counts measured in the 4π bismuth channel is approximated by:

$$Bi_A = \frac{U_{up} - B_o(Z_{STP}) * U_L' - C_o T_L}{\phi_B(Z_{STP}) - B_o(Z_{STP})}$$

where:

U_{up} = Count Rates in Bi channel from 2π detector.

U_L' = Compton Scatter corrected Bi count rate (4π detector).

T_L = Compton Scatter corrected Th count rate (4π detector).

the statistical properties of both R_j and C_j (e.g. the mean and the variance) can be approximated by averaging spatial samples over statistically similar geologic areas rather than by holding j constant, and averaging over time (an obviously impractical procedure).

Let the corrected count rate R_j' be expressed as:

$$R_j' = W * (R_j - C_j) \qquad (1)$$

where W is a set of filter weights convoluted with the corrected count rate:

$$W = (W_{-N}, W_{-N+1}, \ldots W_{-1}, W_0, W_1, \ldots W_{N-1}, W_N)$$

We define a heuristic criterion for determining the statistical adequacy of a given sample:

Let σ be the standard deviation of the correction applied to the raw count rate, and let μ be the statistical average or mean of the correction applied. If R_j represents the count rate (raw data unfiltered) measured at spatial point j, then if the following inequality holds:

$$R_j > C_j + k\sigma;\ C_j = C_j\ (\mu;\ \sigma) \qquad (2)$$

the sample R_j is said to be statistically adequate. The quantity k is an empirically derived constant. Inequality (2) states that the corrected count rate must exceed the uncertainty in the corrections applied to correct the raw counting data. If the corrections were perfectly determined, the inequality (2) simply states that negative count rates are

statistically unreliable (hardly an unexpected result). Applying inequality (2) to equation (1), we have:

$$R'_j + W * (R_j - C_j) > k\sqrt{VAR\ (W * C_j)} \qquad (3)$$

Define the spatial sequence of random variables R and C as:

$$R = (R_o, R_1, \ldots, R_{j-1}, \ldots R_{m-1}, R_m)$$

$$C = (C_o, C_1, \ldots, C_{j-1}, \ldots C_{m-1}, C_m)$$

We assume that both R and C are positive statistically independent random variables. Then, (3) can be written as:

$$R_j' > K\sqrt{W^2_{-N}VAR\ (C_{j-N}) + W^2_{-N+1}VAR\ (C_{j-N+1}) + \overline{\ldots + W_o^2 VAR\ (C_j) + \ldots + W_N^2 VAR\ (C_{j+N})}} \qquad (4)$$

Let us specialize inequality (4) to the determination of statistical reliability for averaged count rate data. We assume that both R and C are Poisson distributed, so that VAR (C_j) = Mean Value of C_j and that VAR (R_j) = $E(R_j)$ = Mean Value of R_j. Since the filtering operation defined by W will always be zero phase shift (i.e. symmetric), then:

$$R_j' > K\sqrt{\mu^2_{-N}\ (E(C_{j-N})) + \mu^2_{-N=1}\ (E(C_{j-N-1}) + E(C_{j+N-1})) + \overline{\ldots + \mu_o^2\ E(C_j)}} \qquad (5)$$

Where $E(C_j)$ is the statistical mean of C determined at point j.

The above inequality is used to ensure the statistical adequacy of averaged or filtered channel data and to ensure that computed ratios using these data are themselves meaningful. Data from Set 5 (Figure 3) are subjected to this criteria. Data failing to meet

this test are flagged on the binary tape for later posting to the export EBCDIC tapes (see Appendix A). A seven-point, central weighted "parabolic" filter was employed to smooth the data prior to testing.

W = (-.09524, .14286, .28571 .33333, .28571, .14286, -.09524)

After the processing of step 5 (Figure 3), the binary tape is merged with the corrected flight line data and next with the edited geological base map data. These steps establish an X-Y (Lat-Long) base for the magnetic and radiometric data, together with the corresponding geologic type for that location.

RADIOELEMENT SENSITIVITY CONSTANTS NORMALIZED TO 400 FEET

SYSTEM #1 - LAMA N49537

Radioelement	Sensitivity Constant
K40	78.46 counts/sec/%
Uranium	9.23 counts/sec/%
Thorium	4.92 counts/sec/%

SYSTEM #2 - LAMA N87638

Radioelement	Sensitivity Constant
K40	88.4 counts/sec/%
Uranium	10.8 counts/sec/ppm eU
Thorium	5.4 counts/sec/ppm eTh

MAGNETIC DATA PROCESSING

Steps in reduction of the magnetic data consisted of diurnal variation correction, common magnetic datum tieing, and removal of regional magnetic fields defined by the International Geomagnetic Reference Field (IGRF).

The IGRF model used to correct the observed data was that adopted by the International Association of Geomagnetism and Aeronomy, Division I study group at Grenoble, France on September 4, 1975. The spherical harmonic coefficients adopted by IAGA were used to generate the theoretical magnetic field at 20 points in each quadrangle. A theoretical least squares polynomial surface in UTM coordinates was then set to fit the theoretical reference field. Letting X = Easting and Y + Northing, the theoretical IGRF field was fitted to a residual error of less than 0.1 gammas by the following series expansion in X and Y:

$$T_{IGRF} = 40060.35 + 0.91443\ (X - 740.73) + 3.8216(Y-2974.4)$$ gammas.

The residual magnetic field (T_{RES}) is defined as:

$$T_{RES} = T_{OBS} - T_{IGRF}$$

where

T_{OBS} is the observed field.

A ground based magnetometer monitored diurnal variations of the magnetic field during the airborne operation. Data

were sampled at 4-second intervals at a sensitivity of one quarter gamma and were recorded along with time code on analogue tapes. Editing was performed to remove data spikes, man-made magnetic events, and extraneous readings. A profile display was made as a check to determine visually that all necessary editing had been performed. The edited, compacted diurnal data were time coded to match the airborne data, (see Figure 3) densified to a one (1) second sample interval and subtracted from the airborne data.

Magnetic differences in the resultant diurnally corrected plots between tie lines and flight lines at intersections were treated by a tieing program. Individual line biases were calculated for both tie and profile lines. These biases were caused by changes of ground based magnetometer location, aircraft magnetization, and effects due to differential aircraft heading.

As a final check on the validity of the magnetic data, a lister plot map was generated and analyzed to locate exceptional tieing and/or location errors.

Both the IGRF and diurnal corrections were then applied to the merged binary tape. This completed the data processing stage of the analysis. Data on the merged binary tape was then ready for display and final presentation.

DATA PRESENTATION

The results of the survey are presented on maps, stacked profiles, and microfilm as follows:

1) Flight path location map - Flight line and tie line paths together with fiducial numbers are plotted for each area on a photo-mosaic base at a scale of 1:24,000.

2) Interpretation map - The magnetic interpretation and the position of uranium anomalies in each area are plotted on a mylar topographic map base on a scale of 1:24,000.

3) Stacked Profiles - Reduced radiometric, magnetic, and ancillary data are presented on profiles vertically stacked relative to a reference line and at a scale of 1:24,000. The following information is presented on these profiles:

   a) Total gamma-ray counts
   b) K40 as percent potassium (%K)
   c) Bi214 as parts per million equivalent uranium (ppm eU)
   d) Tl208 as parts per million equivalent thorium (ppm eTh)
   e) Bi214/Tl208 as ppm eU/ppm eTh
   f) Bi214/K40 as ppm eU/%K
   g) Tl208/K40 as ppm eTh/%K
   h) Total Intensity Magnetic Data
   i) Radar Altimeter

4) Microfilms of the stacked profiles.

DATA INTERPRETATION

INTRODUCTION

Since detailed geologic maps were not available, a preliminary interpretation only of the data was made.

GEOLOGY

Four of the survey areas are in the Upper Peninsular of Michigan, the fifth is in northern Wisconsin. The region is underlain by Precambrian rocks forming the southern extremity of the Canadian Shield. The area has been glaciated, so that much of the bedrock is covered by glacial drift, and rock exposures are confined to the ridges.

Sub-areas A1-A5 (Figure 1) are along the Jacobsville contact, a contact between folded Middle Precambrian metasedimentary and metavolcanic rocks of the Huronian system and undeformed Upper Precambrian sedimentary and volcanic rocks of the Keweenawan system. Conglomerates of the Keweenawan are possible host rocks for uranium deposits.

Area B, Northern Cusmap (Figure 1), is south of the Jacobsville contact, and is underlain by metasedimentary and metavolcanic rocks of the Huronian System.

Area C, Limestone Mountain (Figure 1), is north of the Jacobsville contact, and is underlain by sedimentary and volcanic rocks of the Keweenawan system.

Area D, Sylvania Wilderness area (Figure 1), is south of the Jacobsville contact, and is underlain by metasedimentary and metavolcanic rocks of the Huronian system.

Area E is a wilderness area in northern Wisconsin (Figure 1).

GAMMA-RAY SPECTROMETRIC DATA

The following statistical criteria were used to define a uranium anomaly:

1) Bi214 (eU) - two (2) consecutive averaged eU values each being two (2) or more standard deviations above the mean; or three (3) consecutive averaged eU values, one (1) of which is two (2) or more standard deviations above the mean, and two (2) of which are one (1) or more standard deviations above the mean.

2) Bi214/Tl208 (eU/eTh) - two (2) consecutive averaged eU/Th ratio values which are one (1) or more standard deviations above the mean. To ensure that a high eU/eTh value is not caused by an anomalously low eTh value in the denominator of the ratio, the eTh value must be equal to or greater than (-1) standard deviation from the mean.

Jacobsville Contact Area

Sub-area A1 - Table 1

One uranium anomaly only was found in sub-area 1.

TABLE 1 - URANIUM ANOMALIES IN SUB-AREA A1

ANOMALY #	LINE #	TYPE	NUMBER OF AVERAGED (3X) DATA SAMPLES WITH THE DEFINED DEVIATION FROM THE MEAN								
			-1	0	1	2	3	4	5	6	7
1	2	U	-	-	3	2	-	1	-	-	-

Sub area A2 - Table 2

Five uranium anomalies were found in sub-area 2.

TABLE 2 - URANIUM ANOMALIES IN SUB-AREA A2

ANOMALY #	LINE #	TYPE	NUMBER OF AVERAGED (3X) DATA SAMPLES WITH THE DEFINED DEVIATION FROM THE MEAN								
			-1	0	1	2	3	4	5	6	7
1	10	U	-	-	1	2	-	-	-	-	-
2	14	U	-	-	2	1	-	-	-	-	-
3	19	U	-	-	3	1	-	-	-	-	-
4	TL1	U	-	-	-	2	-	-	-	-	-
5	21	U	-	-	5	12	3	3	2	-	-

Sub-area A3 - Table 3

Seventeen anomalies were found in sub-area 3.

TABLE 3 - URANIUM ANOMALIES IN SUB-AREA A3

ANOMALY #	LINE #	TYPE	NUMBER OF AVERAGED (3X) DATA SAMPLES WITH THE DEFINED DEVIATION FROM THE MEAN								
			-1	0	1	2	3	4	5	6	7
1	29	U	-	-	1	2	-	-	-	-	-
2	50	U	-	-	4	3	-	-	-	-	-
3	50	U	-	-	6	1	1	-	-	-	-
4	21	U	-	-	-	2	-	-	-	-	-
5	TL2	U	-	-	2	1	-	-	-	-	-
6	52	U	-	-	3	1	-	-	-	-	-
7	52	U	-	-	3	1	-	-	-	-	-
8	53	U	-	-	5	1	-	-	-	-	-
9	53	U	-	-	1	2	1	-	-	-	-
10	53	U	-	-	3	2	-	-	-	-	-

11	54	U	-	-	8	6	1	-	-	-	-
12	54	U	-	-	2	1	-	-	-	-	-
13	54	U	-	-	-	3	1	-	-	-	-
14	54	U	-	-	2	1	-	1	-	-	-
15	54	U	-	-	2	1	-	-	-	-	-
16	54	U	-	-	2	2	-	-	-	-	-
17	55	U	-	-	3	1	1	-	-	-	-

Sub-area A4 - Table 4

Twenty uranium anomalies were found in sub-area A4.

TABLE 4 - URANIUM ANOMALIES IN SUB-AREA A4

ANOMALY #	LINE #	TYPE	NUMBER OF AVERAGED (3X) DATA SAMPLES WITH THE DEFINED DEVIATION FROM THE MEAN								
			-1	0	1	2	3	4	5	6	7
1	3	U	-	-	3	1	1	-	-	-	-
2	7	U	-	-	3	1	-	-	-	-	-
3	7	U	-	-	1	-	1	-	-	-	-
4	7	U	-	-	2	1	-	-	-	-	-
5	8	U	-	-	4	1	-	-	-	-	-
6	13	U	-	-	1	2	-	-	-	-	-
7	13	U	-	-	2	1	-	-	-	-	-
8	13	U	-	-	2	1	-	-	-	-	-
9	14	U	-	-	1	2	-	-	-	-	-
10	15	U	-	-	1	2	-	-	-	-	-
11	15	U	-	-	1	2	1	-	-	-	-
12	15	U	-	-	1	2	-	-	-	-	-
13	16	U	-	-	-	2	-	-	-	-	-
14	17	U	-	-	2	1	-	-	-	-	-
15	18	U	-	-	2	-	1	-	-	-	-
16	19	U	-	-	6	3	-	1	1	-	-
17	19	U	-	-	4	2	-	-	-	-	-
18	20	U	-	-	1	2	-	-	-	-	-

19	20	U	-	-	2	3	-	-	-	-	-
20	20	U	-	-	3	1	-	-	-	-	-

Sub-Area A5 - Table 5

Ten uranium anomalies were found in sub-area A5.

ANOMALY #	LINE #	TYPE	NUMBER OF AVERAGED (3X) DATA SAMPLES WITH THE DEFINED DEVIATION FROM THE MEAN								
			-1	0	1	2	3	4	5	6	7
1	3	U	-	-	-	2	-	-	-	-	-
2	4	U	-	-	1	2	-	-	-	-	-
3	6	U	-	-	1	2	-	-	-	-	-
4	9	U	-	-	2	3	1	-	-	-	-
5	10	U	-	-	2	2	1	1	1	-	-
6	11	U	-	-	-	-	1	-	1	-	2
7	12	U	-	-	2	1	5	3	-	-	-
8	12	U	-	-	-	-	1	2	1	-	-
9	27	U	-	-	2	1	2	1	-	-	-
10	27	U	-	-	-	2	-	-	-	-	-

Northern Cusmap - Area B - Table 6

Six uranium anomalies were found in Area B.

ANOMALY #	LINE #	TYPE	NUMBER OF AVERAGED (3X) DATA SAMPLES WITH THE DEFINED DEVIATION FROM THE MEAN								
			-1	0	1	2	3	4	5	6	7
1	1	U	-	-	3	2	-	-	-	-	-
2	2	U	-	-	1	-	-	1	-	-	-
3	TL1	U	-	-	2	1	2	1	-	-	-
4	4	U	-	-	-	-	-	-	-	2	-
5	4	U	-	-	-	-	1	-	-	-	2
6	TL1	U	-	-	1	-	2	-	-	-	2

Limestone Mountain - Area C

No uranium anomalies were found in Area C.

Sylvania Wilderness - Area D

No uranium anomalies were found in Area D.

Wilderness, Wisconsin - Area E

No uranium anomalies were found in Area E.

MAGNETIC DATA

Jacobsville Contact - Sub-areas A1-A5

A number of east-west trending magnetic anomalies are interpreted as due to deep, highly magnetic sources, probably iron formations. Northeast and northwest trending magnetic discontinuities, truncating and off-setting the east-west anomalies, are interpreted as due to faults.

North Cusmap - Area B

A number of east-west trending magnetic anomalies are interpreted as due to deep, highly magnetic sources, probably iron formations. North-south trending magnetic discontinuities, truncating and off-setting the east-west anomalies, are interpreted as due to faults.

Limestone Mountain - Area C

A number of east-west trending magnetic anomalies are interpreted as due to deep, highly magnetic sources, probably iron formations. Northeast trending magnetic discontinuities, truncating and off-

APPENDIX A - TAPE FORMATS

SINGLE RECORD REDUCED DATA TAPE

THE SINGLE RECORD REDUCED DATA TAPE is unlabeled nine track, 2400 foot reel length, NRZI, odd parity. All data are recorded in EBCDIC characters. The two tapes contain identification, header, and data records for the five areas surveyed.
The block length is 6900 characters.
The first physical block on tape is literal alphanumeric listing of the Fortran formats and data items. This listing allows a user to unambigously read and interpret all of the data contained on the tape.
The second physical block is organized as follows:

ITEM	FORMAT	DESCRIPTION
1	A40	AREA NAME AS PROJECT IDENTIFICATION
2	A20	NAME OF SUBCONTRACTOR (HIGH LIFE/QEB)
3	14	APPROXIMATE DATA OF SURVEY (MONTH, YEAR)
4	11	NUMBER OF AERIAL SYSTEMS USED TO COLLECT DATA FOR THIS QUADRANGLE
5	11	AERIAL SYSTEM IDENTIFICATION CODE FOR FIRST SYSTEM
6	A20	AIRCRAFT IDENTIFICATION BY TYPE AND FAA NUMBER FOR FIRST SYSTEM
7	F6.1	NOMINAL ALTITUDE SYSTEM SENSITIVITY RELATIVE TO TERRESTRIAL POTASSIUM (K-40) TO ONE DECIMAL PLACE IN CPS PER PERCENT K FOR FIRST SYSTEM
8	F6.1	NOMINAL ALTITUDE SYSTEM SENSITIVITY RELATIVE TERRESTRIAL URANIUM (BI-214) TO ONE DECIMAL PLACE IN CPS PER PPM EQUIVALENT U

9	F6.1	NOMINAL ALTITUDE SYSTEM SENSITIVITY RELATIVE TO TERRESTRIAL THORIUM (TL-208) TO ONE DECIMAL PLACE IN CPS PER PPM EQUIVALENT TH
10	I6	BLANK FIELD (999999)
11	F6.3	4PI-SYSTEM DATA COLLECTION INTERVAL TO THREE DECIMAL PLACES IN SECONDS FOR FIRST SYSTEM
12	F6.3	2PI-SYSTEM DATA COLLECTION INTERVAL TO THREE DECIMAL PLACES IN SECONDS FOR FIRST SYSTEM
13	I3	NUMBER OF CHANNELS (0-3MeV) IN 4PI SYSTEM FOR FIRST AERIAL SYSTEM
14	I3	NUMBER OF CHANNELS (0-3MeV) IN 2PI SYSTEM FOR FIRST AERIAL SYSTEM
15-24	(SAME)	REPEAT OF ITEMS 5-14 FOR SECOND AERIAL SYSTEM
*	*	*
*	*	*
*	*	*
85-94	(SAME)	REPEAT OF ITEMS 5-14 FOR NINTH AERIAL SYSTEM
95	I3	NUMBER OF FLIGHT LINES ON THIS TAPE
96	I4	FIRST FLIGHT LINE NUMBER ON THIS TAPE
97	I6	FIRST RECORD NUMBER OF FIRST FLIGHT LINE
98	I3	JULIAN DATE (DAY OF YEAR) FIRST FLIGHT LINE DATA WAS COLLECTED
99-101	I4,I6,I3	REPEAT OF ITEMS 96-98 FOR SECOND FLIGHT LINE ON THIS TAPE
*	*	*
*	*	*
*	*	*
390-392	I4,I6,I3	REPEAT OF ITEMS 96-98 FOR 99TH FLIGHT LINE ON THIS TAPE

The third and following physical blocks are organized as follows:

ITEM	FORMAT	DESCRIPTION
1	I1	AERIAL SYSTEM IDENTIFICATION CODE

2	14	FLIGHT LINE NUMBER
3	16	RECORD IDENTIFICATION NUMBER
4	16	GMT TIME OF DAY (HHMMSS)
5	F8.4	LATITUDE TO FOUR DECIMAL PLACES IN DEGREES
6	F8.4	LONGITUDE TO FOUR DECIMAL PLACES IN DEGREES
7	F6.1	TERRAIN CLEARANCE TO ONE DECIMAL PLACE IN METERS
8	F7.1	RESIDUAL (IGRF REMOVED) MAGNETIC FIELD INTENSITY TO ONE DECIMAL PLACE IN GAMMAS
9	A8	SURFACE GEOLOGIC MAP UNIT CODE
10	I4	QUALITY FLAG CODES
11	F6.1	APPARENT CONCENTRATION OF TERRESTRIAL POTASSIUM (K-40) TO ONE DECIMAL PLACE IN PERCENT K
12	F4.1	UNCERTAINTY IN TERRESTRIAL POTASSIUM TO ONE DECIMAL PLACE IN PERCENT K
13	F6.1	APPARENT CONCENTRATION OF TERRESTRIAL URANIUM (BI-214) TO ONE DECIMAL PLACE IN PPM EQUIVALENT U
14	F4.1	UNCERTAINTY IN TERRESTRIAL URANIUM TO ONE DECIMAL PLACE IN PPM EQUIVALENT U
15	F6.1	APPARENT CONCENTRATION OF TERRESTRIAL THORIUM (TL-208) TO ONE DECIMAL PLACE IN PPM EQUIVALENT TH
16	F4.1	UNCERTAINTY IN TERRESTRIAL THORIUM TO ONE DECIMAL PLACE IN EQUIVALENT TH
17	F6.1	URANIUM-TO-THORIUM RATIO TO ONE DECIMAL PLACE IN PPM EQUIVALENT U PER PPM EQUIVALENT TH
18	F6.1	URANIUM-TO-POTASSIUM RATIO TO ONE DECIMAL PLACE IN PPM EQUIVALENT U PER PERCENT K
19	F6.1	THORIUM-TO-POTASSIUM RATIO TO ONE DECIMAL PLACE IN PPM EQUIVALENT TH PER PERCENT K
20	F8.1	GROSS GAMMA (0.4-3.0 MeV) COUNT RATE TO ONE DECIMAL PLACE IN COUNTS PER SECOND
21	F6.1	UNCERTAINTY IN GROSS GAMMA COUNT RATE TO ONE DECIMAL PLACE IN COUNTS PER SECOND

22	F5.1	ATMOSPHERIC BI-214 4PI CORRECTION TO ONE DECIMAL PLACE IN PPM EQUIVALENT U
23	F4.1	UNCERTAINTY IN ATMOSPHERIC BI-214 4PI CORRECTION TO ONE DECIMAL PLACE IN PPM EQUIVALENT U
24	F4.1	OUTSIDE AIR TEMPERATURE TO ONE DECIMAL PLACE IN DEGREES CELSIUS
25	F5.1	OUTSIDE AIR PRESSURE TO ONE DECIMAL PLACE IN MMHG

APPENDIX B - PRODUCTION SUMMARY

USGS - MICHIGAN SURVEY

SYSTEM #1 - N49537

DATE	LINE MILES/REMARKS
09/11/80	75.0 - Area D
09/12/80	Weather/equipment
09/12/80	Weather/equipment
09/12/80	Weather/equipment
09/12/80	Weather/equipment
09/23/80	Weather/equipment
09/24/80	72.0 - Area E
Total	147.0

SYSTEM #2 - N87638

DATE	LINE MILES/REMARKS
10/08/80	218.5
10/09/80	189.25
10/10/80	169.5
10/11/80	Weather
10/12/80	Weather
10/13/80	Weather
10/14/80	132.0
10/15/80	248.5
10/16/80	102.0
10/17/80	Weather
10/18/80	Weather
10/19/80	Weather
10/20/80	Weather
10/21/80	166.5
Total	1226.50